DOI: 10.24352/UB.OVGU-2019-012 TECHNISCHE MECHANIK, 39, 1, (2019), 125 - 137
submitted: July 6, 2018

Smoothed Particle Hydrodynamics for Navier-Stokes Fluid Flow Application

P. Sabrowski, S. Przybilla, F. Pause, L. Beck, J. Villwock, P. U. Thamsen

The aim of this publication is to introduce the particle based computational fluid dynamics (CFD) method smoothed particle hydrodynamics (SPH) and introduce an applicable and valid SPH implementation for practical cases. For this purpose, current research approaches are combined regarding performance and numerical stability.
The principles of the method, the mathematical basics and the discretization of the Navier-Stokes equations are clarified. Furthermore, the implementation of method-specific boundary conditions, wall, inlet and outlet, as well as several correction procedures and a surface tension setup into the present code framework are described.
The advantages and validity of the method are shown based on different cases. The free surface fluid behavior of a dam break is compared to experimental data of the time dependent water level of selected positions. A Karman vortex street is validated by its Strouhal number for different Reynolds numbers. The frequency of an oscillating drop is analysed and compared to the analytical solution.
The SPH is utilized for pipe flows influenced by a backward facing step and shows an expected qualitative flow field.

1 Introduction

The method smoothed particle hydrodynamics is particle based and has its origin in the applications of astrophysics (Gingold and Monaghan, 1977; Lucy, 1977). Today, it is efficiently applied for liquid flows. A frequently used form is the weakly compressible smoothed particle hydrodynamics (WCSPH). It treats fluids as stiff media and adds an equation of state.
Due to the meshfree properties, the main advantage of the method is the simple applicability to free surface flows, moving geometries and multiphase phenomena. Where classical CFD methods usually require dynamic remeshing, SPH benefits from its Lagrangian definition. Due to its high parallelization capability, it is well suited for high performance computing (Braun et al., 2017).
Nevertheless, SPH still has some deficiencies. Although there are several working approaches of modelling turbulence, it is still a present research topic. Another feature that is still in development is the variable resolution in predefined areas, as adaptive refinements. For the implementation splitting and merging algorithms are utilized. The most advanced approaches are given by Vacondio et al. (2016) and Chiron et al. (2017). In some cases, boundary conditions may cause undesired behavior, for instance penetrations in wall BCs or backflows for inlet and outlet BCs (Tafuni et al., 2017). Another aspect is the existing proof of convergence which only holds for regular distributed particles (Violeau, 2012).
Due to the efficient approximation of the Navier-Stokes equations, especially for free surface flows, SPH has its primary application fields in coastal flows and atomization processes, among others. A typical SPH application that stems from the advantages in simulating complex and moving geometries are gear boxes.
The goal of this work is to introduce an applicable and valid SPH tool for practical cases. Hence, the most promising results of the latest SPH research are combined regarding performance and numerical stability. For this purpose, latest open and wall boundary approaches are implemented into the present code framework and enhanced as well as numerical stabilizing methods.
This software framework, the utilized models and their advantages are expounded as a foundation for the subsequent work in the field of wastewater treatment. The simulation of waste water systems and optimization of pump stations regarding sedimentation is a research topic that stems from the EFRE funded project OPuS (“Optimization of pump stations due to the Simulation of Sedimentation Processes”) at Beuth University of Applied Sciences.

2 Physical Model

The Lagrangian form of the Navier-Stokes equations is used to describe the fluid flow, with the mass balance in Eq. (1) and the momentum balance in Eq. (2)

$$\frac{d\rho}{dt} = -\rho\nabla\cdot\underline{v}, \tag{1}$$

$$\frac{d\underline{v}}{dt} = \frac{1}{\rho}\left(-\nabla p + \mu\nabla^2\underline{v}\right) + \underline{g}, \tag{2}$$

where ρ and p are density and pressure, $\underline{v}$ and $\underline{g}$ are velocity and gravitational acceleration. μ denotes the dynamic viscosity of the fluid.

Weakly compressible smoothed particle hydrodynamics (WCSPH) is often used to model incompressible fluids. For the weakly compressible behavior an equation of state is necessary. The Cole equation describes water as a stiff medium and is usually utilized in SPH (Monaghan, 1994)

$$p = \frac{\rho_0 c^2}{\gamma}\left(\left(\frac{\rho}{\rho_0}\right)^{\gamma} - 1\right) + p_0. \tag{3}$$

The material parameter γ is set to 7 for water (Cole, 1948). c is the speed of sound, ρ_0 the reference density and p_0 the background pressure. When acoustics can be neglected, an artificial speed of sound is often introduced. This allows the increase of the time step without degrading the quality of the result. Usually a change in density of 1% is permitted which leads to an artificial speed of sound ten times bigger than the maximum expected velocity. The letter can be derived by an educated guess or simpler analytical approaches such as Torricelli's law (Monaghan, 1992).

Modelling turbulence is a not yet a mature discipline using SPH. Next to costly direct numerical simulations (DNS), large eddy simulations (LES) were introduced to SPH (Adami et al., 2013; Dalrymple and Rogers, 2006). A more practical approach to industrial application involves Reynolds-averaged Navier-Stokes (RANS) models based on a first-order eddy viscosity closure (Violeau, 2004). A detailed overview of turbulence modelling in SPH was presented by Violeau and Rogers (2016).

An alternative approach is the incompressible smoothed particle hydrodynamics (ISPH) method were incompressible fluids and therefore divergence free velocity fields are handled. This introduces necessary iterative solving procedures (Cummins and Rudman, 1999).

3 Numerical Model

In 1992, Monaghan (1992) successfully applied SPH to fluid dynamics. The mesh-free method is based on smoothing physical fields and their gradients at defined particle positions.

Using the Dirac delta distribution δ, every value of a continuous function f can be described at a position $\underline{r}$ in Ω through the following convolution integral:

$$f(\underline{r}_i) = (\delta * f)(\underline{r}_i) = \int_{\Omega} f(\underline{r})\delta(\underline{r}_i - \underline{r})d\Omega, \qquad \forall\underline{r} \in \Omega \tag{4}$$

Thereby, the Dirac delta distribution holds the following characteristics:

$$\delta(\underline{r} - \underline{r}_i) = \begin{cases} \infty, & \underline{r} = \underline{r}_i \\ 0, & \underline{r} \neq \underline{r}_i \end{cases}, \tag{5}$$

$$\int_{\Omega} \delta(\underline{r})d\Omega = 1. \tag{6}$$

In SPH the Dirac delta distribution is approximated by the so-called kernel function w_h. It must satisfy specific requirements, see Eqs. (7) to (9). The third property limits interpolation consistency to an order of one (Violeau, 2012).

$$\lim_{h\to 0} w_h = \delta, \tag{7}$$

$$\int_{\Omega} w_h(\underline{r})d\Omega = 1, \tag{8}$$

$$w_h(\underline{r}) \geq 0, \qquad \forall \underline{r} \in \Omega. \tag{9}$$

The simplest kernel function is the Gaussian. The introduced solver on the other hand uses the Wendland kernel shown in Eq. (10) is used,

$$\begin{gathered} w_h\left(\underline{r}_{ij}\right) = w_h(r_{ij}) = \frac{\alpha_d}{h^d}\begin{cases}\left(1-\frac{r_{ij}}{2h}\right)^4\left(1+\frac{2r_{ij}}{h}\right), & \frac{r_{ij}}{h} \in [0,2] \\ 0, & else\end{cases} \\ \left(r_{ij} = \left\|\underline{r}_i - \underline{r}_j\right\|, \underline{r}_{ij} = \underline{r}_i - \underline{r}_j, \qquad i,j = 1,\dots,n\right), \end{gathered} \tag{10}$$

where d is the number of dimensions, h is the smoothing length, α_d is a dimension dependent constant factor (Wendland, 1995). The underlying interpolation procedure is demonstrated in Figure 1.

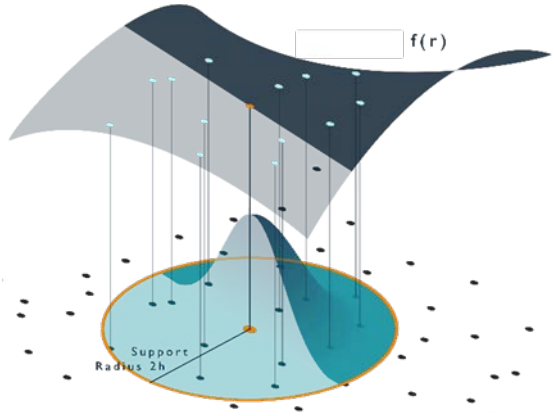

Figure 1. Reference and actual configuration of a binary mixture (Sabrowski et al., 2017)

The next step is the discretization of the integral in Eq. (4) through a Riemann sum. n is the number of particles, N the number of neighbour particles, m_j is the mass and ρ_j the density of neighbour particle j

$$[f]_d(\underline{r}_i) = \sum_{j=1}^{N} \frac{m_j}{\rho_j} f(\underline{r}_j) w_h(r_{ij}). \tag{11}$$

Applying the SPH methodology to the Navier-Stokes equations leads to a system of ordinary differential equations (ODE). For the discretization a representation of the gradient, divergence and Laplacian is required. To determine the gradient in the simplest SPH manner the interpolation described above is applied on the gradient of a sufficiently smooth function f. Together with partial integration the following identity holds

$$\nabla f(\underline{r}_i) = \int_\Omega \nabla f(\underline{r}) w_h(\underline{r}_i - \underline{r}) d\Omega = \int_{\partial\Omega} f(\underline{r}) w_h(\underline{r}_i - \underline{r}) \underline{n}(\underline{r}) d\Gamma - \int_\Omega f(\underline{r}) \nabla w_h(\underline{r}_i - \underline{r}) d\Omega \tag{12}$$

Assuming the point $\underline{r}_i$ is not close to $\partial\Omega$, the surface integral vanishes due to the compact support of w_h. With the identity $\nabla_i w_h(\underline{r}_i - \underline{r}) = -\nabla w_h(\underline{r}_i - \underline{r})$ the gradient can thus be rewritten as

$$\nabla f(\underline{r}_i) = \int_\Omega f(\underline{r}) \nabla_i w_h(\underline{r}_i - \underline{r}) d\Omega. \tag{13}$$

This generic calculation can equally be applied to the divergence and results for sufficiently smooth g in

$$\nabla \cdot \underline{g}(\underline{r}_i) = \int_\Omega \underline{g}(\underline{r}) \cdot \nabla_i w_h(\underline{r}_i - \underline{r}) d\Omega. \tag{14}$$

Now this continuous representation can be spatially discretized. With additional algebra, more formulations for the differential operators can be derived (Watkins et al., 1996). These formulations hold properties that make them advantageous over the formulation above. The most frequently used formulations are the so-called symmetric divergence

$$\nabla \cdot \underline{g}_i = -\frac{1}{\rho_i}\sum_{j=0}^{N} m_j \underline{g}_{ij} \cdot \nabla_i w_h(r_{ij}) \tag{15}$$

and the anti-symmetric gradient operator

$$\nabla f_i = \rho_i \sum_{j=0}^{N} m_j \left(\frac{f_i}{\rho_i^2} + \frac{f_j}{\rho_j^2}\right) \nabla_i w_h(r_{ij}). \tag{16}$$

The continuity and the momentum equation are examined separately using the advantages of the different discretization schemes available for the differential operators. The divergence in the continuity equation is usually determined by the symmetric operator due to its improved mathematical consistency (Violeau, 2012)

$$\nabla \cdot \underline{v}_i = -\frac{1}{\rho_i}\sum_{j=1}^{n} m_j (\underline{v}_i - \underline{v}_j) \cdot \nabla_i w_h(r_{ij}). \tag{17}$$

On the contrary, the anti-symmetric formulation is used to describe the pressure gradient in the momentum equation because of its favorable strict conservation of linear and angular momentum guaranteed by this operator (Monaghan, 1988)

$$\nabla p_i = \rho_i \sum_{j=1}^{n} m_j \left(\frac{p_i}{\rho_i^2} + \frac{p_j}{\rho_j^2}\right) \nabla_i w_h(r_{ij}). \tag{18}$$

To model the viscous term, many approaches exist. The most obvious idea is to use the operators derived above and apply the divergence on the gradient operator. This comes with a high computational overhead and leads to inaccurate velocity fields (Watkins et al., 1996). Instead the viscous operator by Monaghan and Kos (1999) is used in this work

$$\nu \Delta \underline{v}_i = \sum_{j=1}^{n} \frac{4(d+2) m_j \nu \underline{v}_{ij} \cdot \underline{r}_{ij}}{(\rho_i + \rho_j)({r_{ij}}^2 + (0.1h)^2)} \nabla_i w_h(r_{ij}). \tag{19}$$

It conserves linear and angular momentum while introducing an artificial bulk viscosity. Another frequently used approach is based on a finite differences gradient coupled with a SPH divergence formulation (Morris et al., 1997). The resulting system of ODEs reads as follows:

$$\frac{d\rho_i}{dt} = \sum_{j=1}^{n} m_j (\underline{v}_i - \underline{v}_j) \cdot \nabla w_h(r_{ij}), \tag{20}$$

$$\frac{d\underline{v}_i}{dt} = -\sum_{j=1}^{n} m_j \left(\frac{p_i}{\rho_i^2} + \frac{p_j}{\rho_j^2} - \frac{4(d+2)\nu \underline{v}_{ij} \cdot \underline{r}_{ij}}{(\rho_i + \rho_j)({r_{ij}}^2 + \eta^2)}\right) \nabla_i w_h(r_{ij}) + \underline{f}_i. \tag{21}$$

where $\underline{f}_i$ includes external accelerations like gravity and $\eta = 0.1h$ is introduced to avoid zero nominators. Instead of utilizing the continuity equation the density can be computed directly using the SPH identity (Monaghan, 1992)

$$\rho_i = \sum_{j=1}^{n} m_j w_h(r_{ij}). \tag{22}$$

Using this identity saves an additional step in the time integration scheme and gives good results applied to particles inside the fluid. Close to the surface, however a non-negligible error is introduced by the truncated kernel support and it thus needs special consideration when applied (Morris et al., 1997).

To advance in time, the system of ODEs achieved by the SPH discretization can be solved by any time integration scheme. The explicit nature of WCSPH leads to small timesteps and as a result, many timesteps have to be computed. To reduce the introduced error, it is beneficial to use a symplectic scheme (Violeau, 2012). In this work the velocity Verlet scheme (Swope et al., 1982) is used adjusted by the additional density equation as follows:

$$\begin{aligned}
\underline{v}\left(t+\frac{\Delta t}{2}\right) &= \underline{v}(t)+\frac{\Delta t}{2}\frac{d\underline{v}}{dt}(t),\\
\underline{r}\left(t+\frac{\Delta t}{2}\right) &= \underline{r}(t)+\frac{\Delta t}{2}\underline{v}\left(t+\frac{\Delta t}{2}\right),\\
\rho(t+\Delta t) &= \rho(t)+\Delta t\frac{d\rho}{dt}\left(t+\frac{\Delta t}{2}\right),\\
\underline{r}(t+\Delta t) &= \underline{r}\left(t+\frac{\Delta t}{2}\right)+\frac{\Delta t}{2}\underline{v}\left(t+\frac{\Delta t}{2}\right),\\
\underline{v}(t+\Delta t) &= \underline{v}\left(t+\frac{\Delta t}{2}\right)+\frac{\Delta t}{2}\frac{d\underline{v}}{dt}(t+\Delta t).
\end{aligned} \tag{23}$$

To dynamically determine the timestep, the well-known CFL condition is applied (Courant et al., 1929)

$$\Delta t \leq \omega_1 \frac{h}{c}. \tag{24}$$

In addition, two more conditions are used to take the current acceleration and viscosity in consideration (Morris et al.,1997)

$$\Delta t \leq \omega_2 \sqrt{\frac{h}{\max\limits_{i=1,\dots,n}\left(\left\|\frac{d\underline{v}_i}{dt}\right\|\right)}}, \tag{25}$$

$$\Delta t \leq \omega_3 \frac{h^2}{\max\limits_{i=1,\dots,n} \nu_i}. \tag{26}$$

Typical values are $\omega_1 = 0.25$, $\omega_2 = 0.25$, $\omega_3 = 0.125$. The new timestep is the maximal timestep that holds for all three conditions.

To guarantee more stable pressure fields and closely fitted fluid particles near the boundary, the boundary condition proposed by Adami et al. (2012) is utilized. It is based on the pressure extrapolation from surrounding fluid particles and has the claim to ensure $\nabla p = 0$. This approach allows the proper modelling of wall boundaries.
The implemented inlet and the outlet boundary condition are also based on this pressure interpolation principle. The inlet pressure interpolation works exactly like the boundary condition by Adami et al. (2012). For the outlet, a particle is defined as a slave particle when undercutting a defined distance from predefined fixed outlet particles. For those slave particles, the pressure is interpolated from fluid and outlet. While the outlet particles hold a pre-defined pressure. As soon as slave particles leave the outlet zone, they are deleted.
To reduce the noise in the pressure field a numerical diffusive term proposed in Antuono et al. (2010) is applied on the density calculation, hence a smoothed pressure field and makes SPH applicable for violent water flows (Marrone et al., 2011).

For several approaches a surface tracking algorithm is necessary. The technique used here is introduced by He (2014) as the gradient of the color function, defined as $c = 1$ for each particle. The color gradient ∇c_i is defined as

$$\nabla c_i = \frac{\sum_j V_j \nabla_i w_h(r_{ij})}{\sum_j V_j w_h(r_{ij})}, \tag{27}$$

where V_j denotes the volume of particle j. The expected value within a fluid field is approximately zero and significantly greater at a free surface. Consequently, a limit value can be defined to identify the surface particles. Other surface tracking approaches are shown by Lind et al. (2012) and Marrone et al. (2010).

After a surface tracking is established, an interface-based surface tension model can be implemented. Here, the continuum surface force by Brackbill et al. (1992) is chosen. It is based on the surface tension coefficient σ, the surface curvature κ, the inwards surface normal $\underline{n_s}$, and the surface delta function δ_Σ. The resulting surface force $\underline{f_s}$ reads as follows:

$$\underline{f_s} = \sigma \kappa \underline{n_s} \delta_\Sigma \tag{28}$$

with

$$\delta_\Sigma = |\nabla c|, \tag{29}$$

$$\underline{n_s} = \frac{\nabla c}{|\nabla c|}. \tag{30}$$

The surface curvature κ of particle i can be determined by the SPH divergence operator (Adami et al., 2010):

$$\kappa_i = -\nabla \cdot \underline{n}_i = d \frac{\sum_j (\underline{n}_i - n_j) \mathrm{V_j} \nabla_\mathrm{i} w_h(r_{ij})}{\sum_j r_{ij} V_j |\nabla_\mathrm{i} w_h(r_{ij})|}. \tag{31}$$

These forces can lead to instabilities that introduce particle clustering and therefore affects the mathematical consistency.
Latter can only be proved for an even particle distribution (Violeau, 2012). Therefore, various particle reordering approaches were developed. A generalized shifting technique was introduced by Lind et al. (2012) derived from Fickian diffusion. A small perturbation term $\delta \underline{v_i}$ is added to the Lagrangian velocity $\underline{v_i}$with $\delta \underline{v_i} \ll \underline{v_i}$

$$\underline{v_i^*} = \underline{v_i} + \delta \underline{v_i}, \tag{32}$$

where $\delta \underline{v_i}$ is defined as

$$\delta v_i := \begin{cases} -\underline{v_{char}} 2h \underline{n} & , \quad \underline{v_{char}} 2h \|\underline{n}\| < 0.25 \|\underline{v_i}\| \\ -0.25 \|\underline{v_i}\| \dfrac{\underline{n}}{\|\underline{n}\|} & , \quad else \end{cases}, \tag{33}$$

according to Oger et. al. (2015), where $\underline{n} = \sum_j \nabla_i w_h(r_{ij}) V_j$. Sun et. al. (2017b) suggests a shifting distance restriction of 5 percent of the particle diameter Δx_i.

To exclude surface particles from shifting the previously described surface tracking algorithm is utilized.
Particle properties like mass and pressure are shifted with the particle position. Therefore, mass and momentum conservation cannot be guaranteed. Oger et. al. (2015) introduces an Arbitrary Lagrangian Eulerian scheme which allows mass fluxes between particles and ensures mass and momentum conservation.

4 Validation on Standard Cases

The dam break is defined by the SPH European Research Interest Community (SPHERIC) as one of the SPH benchmark tests and is therefore used to validate the SPH free surface flow prediction. The experimental setup and the results are specified in Issa and Violeau (2006). Kleefsman (2005) provides the experimental data to which the present implementation is compared to. There, the water height is determined over time at four different positions. Figure 2 shows the case setup and the two considered water level sensors *H1* and *H2* similarly to the experimental data. Additionally, it visualizes the fluid field at time $t = 0.8\ s$. The tank has a height of 3.22 m and a length of 1 m. The initial water block has a height of 0.55 m and a length of 1.228 m. It is positioned on the left corner of the tank. As soon as the simulation begins, water dam breaks and crushes into an obstacle of 0.161 m height and width. It is located at 2.476 m distance from the left tank wall.

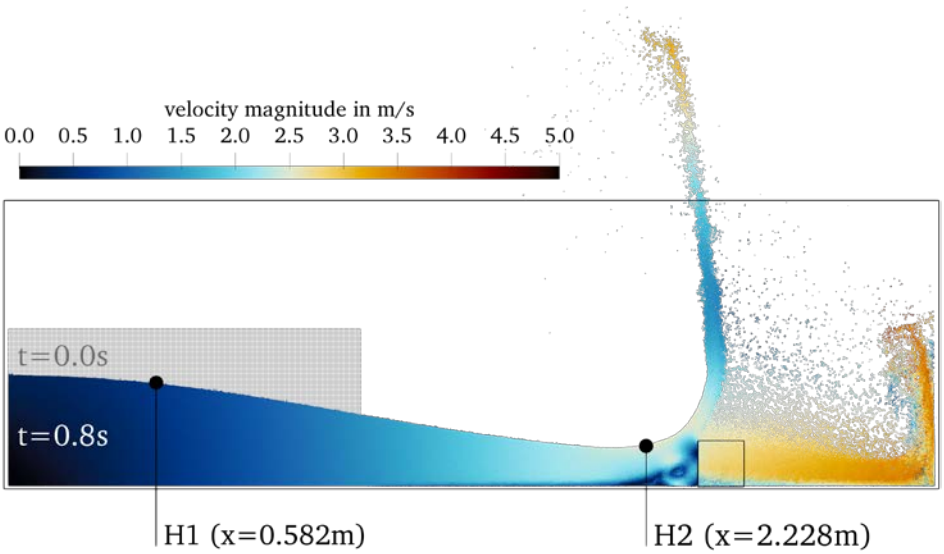

Figure 2. Velocity field for the dam break case

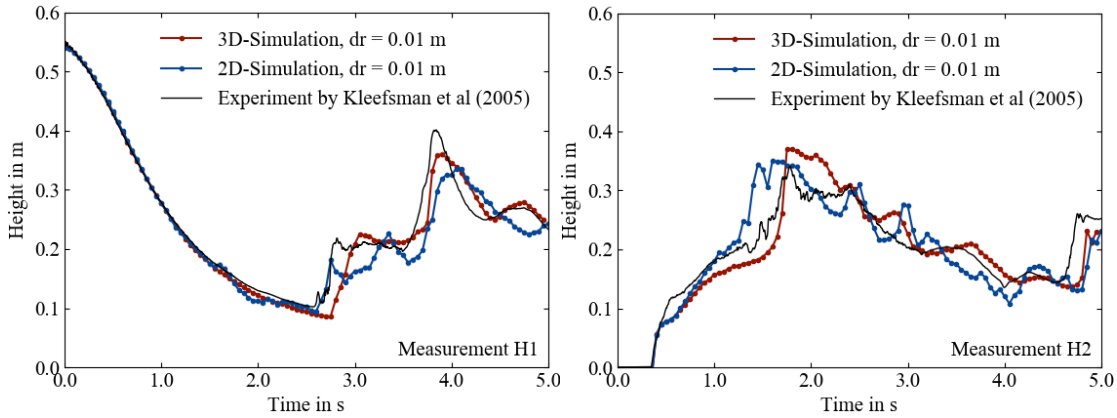

Figure 3. Variation of the water level with time at the height sensors

Figure 3 shows that the water levels resulting from the simulation are in good agreement with the experimental data. The deviations in the 2D case result from neglecting the interspaces between obstacle and wall. Moreover, turbulence modelling is not included which also causes a discrepancy to the measurements.
Nevertheless, the results of the case indicate SPH to be a suitable method for simulating highly dynamic free surface flow.

To evaluate external flows, the Karman vortex street is investigated. Although, it is not perfectly fitted to be a favorable SPH case, it can be used to validate the capabilities of SPH. For Reynolds number 100 and 200 the Strouhal number calculated from the vortex shedding frequency is determined for the present implementation which includes the incorporation of open and wall boundaries next to numerical stabilization. No-slip is used for the cylinder surface, slip for the upper and lower calculation space and open boundaries for the left and right in and outflow. Results are compared to numerical and experimental data from literature, see Table 1.
Figure 4 shows the formation of vortices with initially position-dependent marked particles.

Figure 4. Karman vortex street (position marked particles)

The frequency is examined based on a Fast Fourier Transformation on the *y*-velocity median for a fixed *x* position. The Strouhal number St can be calculated by

$$St = \frac{f_v d_c}{v}. \tag{34}$$

where f_v denotes the shedding frequency and d_c the obstacle diameter. Table 1 shows the results for Reynolds number 100 and 200 of the present work, experimental measurements by Roshko (1954) and numerical results by the references mentioned below.

Table 1. Comparison of Strouhal number with experimental and numerical data

Source	**St (Re=100)**	**St (Re=200)**
Present work	0.174	0.207
Roshko (1954)	0.170	0.185
Tafuni (2016)	0.174	0.205
Calhoun (2002)	0.175	0.202
Liu et al. (1998)	0.165	0.192

The simulation values for both Reynolds numbers show a good agreement with literature data, although the Strouhal number for Reynolds number 200 is determined higher than the compared literature values. Sun et al. (2017a) ascertain that higher Reynolds numbers cause more negative vortex pressures and therefore a less accurate representation of the physical phenomenon. Sun et al. (2017a, b) introduce approaches to avoid negative pressures which will be investigated prospectively.

Lastly, an oscillating droplet with free surface is analysed. Hence, the surrounding air is not calculated. Here, the relative pressure Δp and the oscillation frequency f of the SPH droplet simulation is compared to analytical solutions. Both are determined for a variety of particle radii R.
The analytical pressure can be determined by (Urso, 1999)

$$\Delta p = \frac{R}{\sigma} \tag{35}$$

and the oscillation frequency (Rayleigh, 1879) by

$$f = \left(2\pi\sqrt{\frac{R^3\rho}{6\sigma}}\right)^{-1} \tag{36}$$

The initial condition of the oscillating droplet and its pressure distribution can be seen in Figure 5. The particles position is initialized on a cartesian grid. As soon as the particles are set in motion, the particles distribution is uniform but less systematic. Especially at the surface, the distribution shows a characteristic but less uniform behaviour. This could influence the mathematical consistency at the surface which would also cause problems in of the physical field. The pressure field quality at the surface confirms the suspicion. The pressure values at the surface are comparatively noisy. Nevertheless, the pressure results within the droplet are in good agreement with the analytical solutions, see Figure 6. The same applies for the comparison of the simulated oscillation frequency.

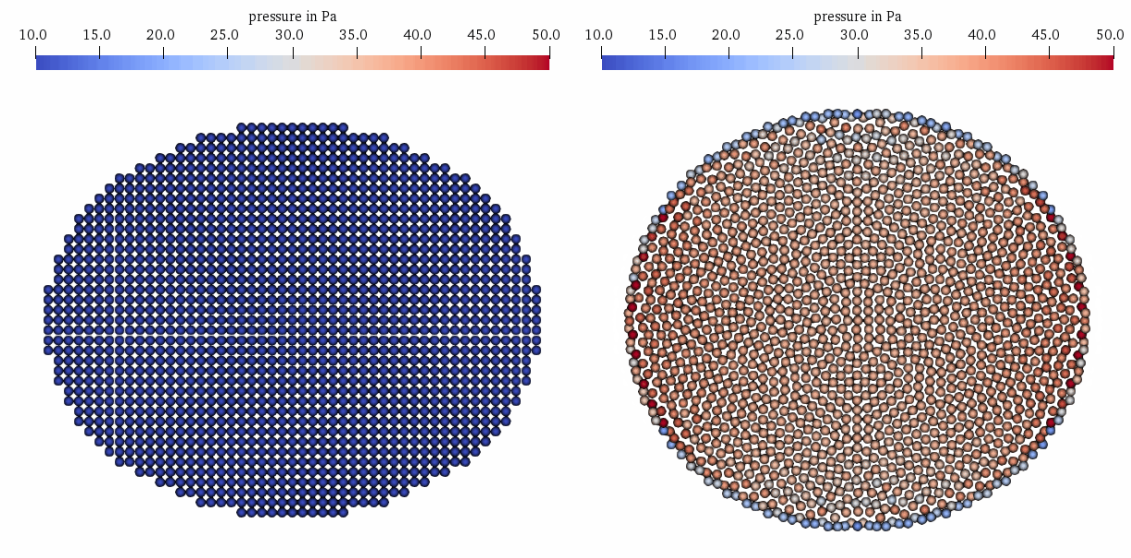

Figure 5. Initial (left) and rearranged (right) particle configuration and pressure distribution of an oscillating droplet

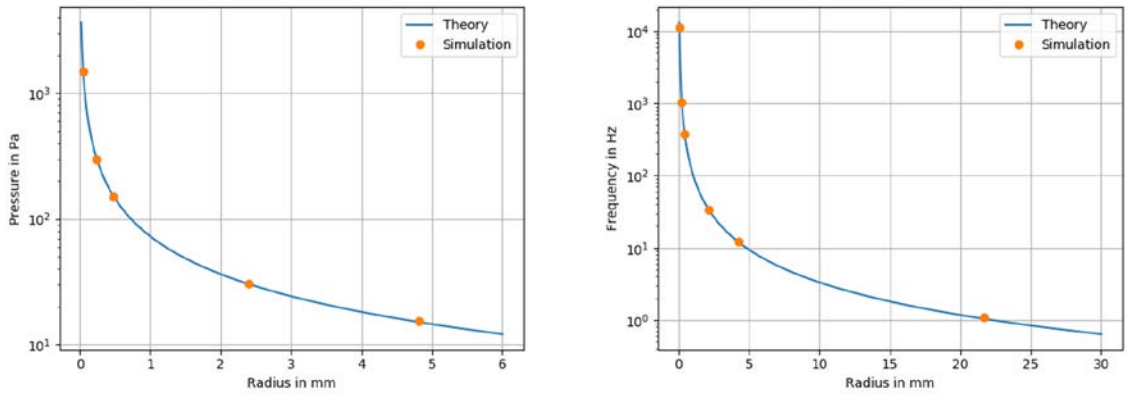

Figure 6. Comparison of analytical and numerical internal pressure (left) and oscillation frequency (right) of a droplet using WCSPH simulation

5 Application Feasability

The EFRE funded research project OPuS at Beuth University of Applied Sciences aims to optimize the geometry of wastewater systems and prevent sedimentary deposition. As a first step, a simplified experimental setup was built at Technische Universität Berlin to investigate flow and sedimentation phenomena in pipes with different inline components. Here, the applicability of the shown methodological software setup is examined as a first feasibility study to assess the occurring physical phenomena and stability. The described test rig with a backward facing step, see Figure 7, is utilized with a length of 85.5 cm between inlet and outlet, a maximum height of 16 cm and a step of 4 cm.

The presented implementation provides all necessary functionalities to approach this setup.

Figure 7 shows the pressure field in the backward facing step. The introduced open boundaries at the inlet and outlet avoid reflections of internal pressure waves, which in the past caused unphysical resonance effects. Furthermore, the wall boundary condition and the density diffusion term improve the pressure field significantly.

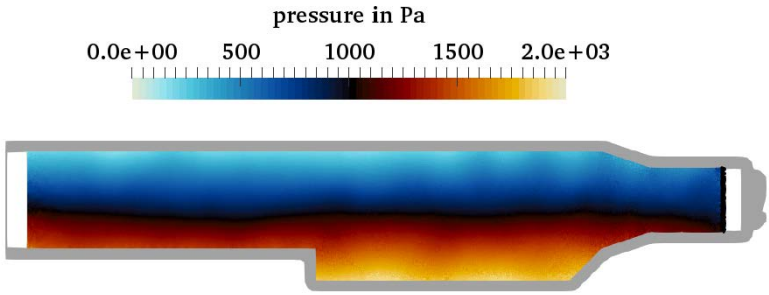

Figure 7. Pressure field of the backward facing step

A first glimpse at the vortex, which is induced by the velocity field at the backward facing step, shows the expected characteristics, see Figure 8. The vorticity and the dimensioning of the occurring flow phenomena will be further analysed in future work.

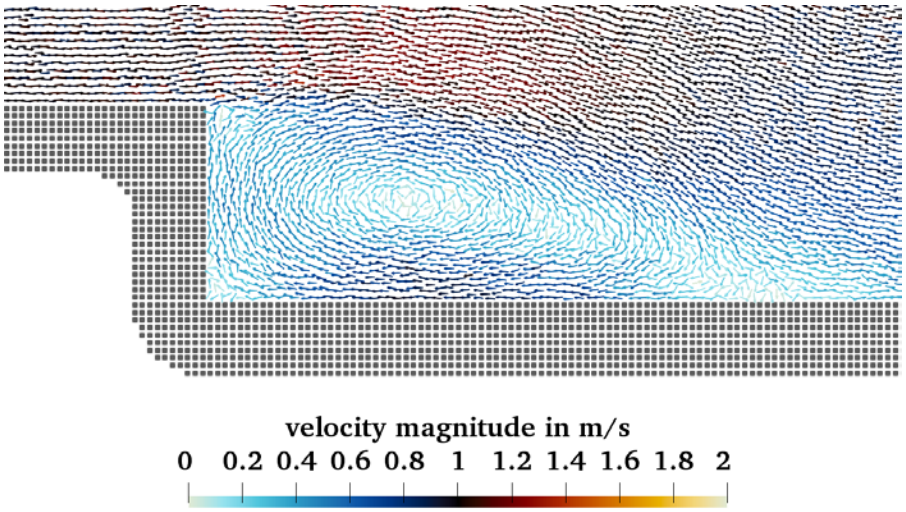

Figure 8. Velocity field of the backward facing step

Building on those approaches, the velocity field will be validated by comparing to experimental particle image velocimetry measurements.

6 Conclusion and Perspective

In this work a combined implementation of several of the latest approaches and improvements in the field of SPH is presented to allow the challenging of real world flow problems. It was possible to validate the incorporation of density diffusion schemes, improved wall treatments and the extension of the wall boundary consideration to open boundary problems for violent free surface flows as well as on an internal flow case.
The simulations of the validation cases are in good agreement with literature and experimental data. Simulations that involve free surface flows as well as external and internal flows were observed to validate the numerical quality of SPH. First pipe simulations are promising for future industrial applications.
Based on the displayed work performed with the described software setup, the application of pipe flow with varying internal features will be continued and compared to data of a corresponding experimental setup. To guarantee the necessary performance, an MPI framework will be established. Especially the pipe flow, adaptive refinements will be further developed to increase resolution in several areas of interest. Moreover, the mentioned turbulence models will further be investigated. To reach the aims of the project, a multiphase and a sedimentation model will be included and geometry studies for avoiding sedimentation in pump stations will be performed.

Acknowledgments

The presented results were established in the EFRE funded research project OPuS at Beuth University of Applied Sciences in close cooperation with Technical University Berlin using the software dive.sph. We want to thank all supporters to our research work.

References

Adami, S.; Hu, X. Y.; Adams, N. A. A new surface-tension formulation for multi-phase SPH using a reproducing divergence approximation. *Journal of Computational Physics*, 229, (2010), 5011–5021.

Adami, S.; Hu, X. Y.; Adams, N. A.: A generalized wall boundary condition for smoothed particle hydrodynamics. *Journal of Computational Physics*, 231, (2012), 7057-7075.

Adami, S.; Hu, X. Y.; Adams, N. A.: Simulating 3D turbulence with SPH. *8th International SPHERIC Workshop*, (2013), 377-382.

Antuono, M.; Colagrossi, A.; Marrone, S.; Molteni, D.: Free-surface flows solved by means of SPH schemes with numerical diffusive terms. *Computer Physics Communications*, 181, (2010), 532-549.

Braun, S.; Holz, S.; Wieth, L.; Dauch, T. F.; Keller, M. C.; Chaussonnet, G.; Schwitzke, C.; Bauer, H.-J.: HPC Predictions of Primary Atomization with SPH: Validation and Comparison to Experimental Results. *12th International SPHERIC Workshop*, (2017), 314-321.

Brackbill, J.; Kothe, S.; Zemach, C.: A continuum method for modeling surface tension. *Journal of Computational Physics*, 100, (1992), 335–354.

Calhoun, D.: Cartesian Grid Method for Solving the Two-Dimensional Streamfunction-Vorticity Equations in Irregular Regions. *Journal of Computational Physics*, 176, (2002), 231-275.

Chiron, L.; Oger, G.; de Leffe, M.; Le Touzé, D.: Analysis and improvements of Adaptive Particle Refinement (APR) through CPU time, accuracy and robustness considerations. *Journal of Computational Physics*, 354, (2017), 552-575.

Cole, H. R.: *Underwater Explosions*. Princeton University Press, Princeton (1948).

Courant, R.; Friedrichs, K.; Lewy, H.: Über die partiellen Differenzengleichungen der mathematischen Physik. Mathematische Annalen, 100, (1929), 32–74.

Cummins, S. J.; Rudman, M.: An SPH Projection Method. *Journal of Computational Physics*, 152, (1999), 584-607.

Dalrymple, R. A.; Rogers, B. D.: Numerical modeling of water waves with the SPH method. *Coastal Engineering*, 53, (2006), 141-147.

Gingold, R. A.; and Monaghan, J. J.: Smoothed particle hydrodynamics:theory and application to non-spherical stars. *Monthly Notices of the Royal Astronomical Society*, 181, (1977), 375-389.

He, X.; Wang, H.; Zhang, F.; Wang, H.; Wang,G.; Zhou, K.: Robust Simulation of Small-Scale Thin Features in SPH-based Free Surface Flows, *ACM Transactions on Graphics*. 34, (2014), 1-9.

Issa, R.; Violeau, D.: Test-case 2 3D dambreaking. *ERCOFTAC, SPH European Research Interest Community SIG*, Electricité De France, Laboratoire National d'Hydaulique et Environnement, (2006).

Kleefsman, K. M. T.; Fekken, G.; Veldman, A. E. P.; Iwanowski, B.; Buchner, B.: A Volume-of-Fluid based simulation method for wave impact problems. *Journal of Computational Physics.* 206, (2005), 363-393.

Lind, S. J.; Xu, R.; Stansby, P. K.; Rogers, B. D.: Incompressible smoothed particle hydrodynamics for free-surface flows: A generalised diffusion-based algorithm for stability and validations for impulsive flows and propagating waves. *Journal of Computational Physics.* 231, (2012), 1499-1523.

Liu, C.; Zheng, X.; Sung, C. H.: Preconditioned Multigrid Methods for Unsteady Incompressible Flows. *Journal of Computational Physics*, 139, (1998), 35-57.

Lucy, L. B.: A numerical approach to the testing of the fission hypothesis. *Astronomical Journal*, 82, (1977), 1013-1024.

Marrone, S.; Antuono, M.; Colagrossi, A.; Colicchio, G.; Le Touzé, D.; Graziani, G.: δ-SPH model for simulating violent impact flows. *Computer Methods in Applied Mechanics and Engineering*, 200, (2011), 1526-1542.

Marrone, S.; Colagrossi, A.; Le Touzé, D.; Graziani, G.: Fast free-surface detection and level-set function definition in SPH solvers. *Journal of Computational Physics.* 229, (2010), 3652-3663.

Monaghan, J. J.: An introduction to SPH. *Computer Physics Communications*, 48, (1988), 89-96.

Monaghan, J. J.: Smoothed Particle Hydrodynamics. *Annual Review of Astronomy and Astrophysics*, 30, (1992), 543-574.

Monaghan, J. J.: Simulating Free Surface Flows with SPH. *Journal of Computational Physics*, 110, (1994), 399-406.

Monaghan, J. J.; Kos, A.: Solitary Waves on a cretan beach. *Journal of Waterway, Port, Coastal, and Ocean Engineering*, 125, (1999), 145-155.

Morris, J. P.; Fox, P. J.; Zhu, Y.: Modeling Low Reynolds Number Incompressible Flows Using SPH. *Journal of Computational Physics*, 136, (1997), 214-226.

Oger, G.; Marrone, S.; Le Touzé, D.; de Leffe, M.: SPH accuracy improvement through the combination of a quasi-Lagrangian shifting transport velocity and consistent ALE formalisms. *Journal of Computational Physics*. 313, (2016), 76-98.

Rayleigh, L.: On the Capillary Phenomena of Jets. *Proceedings of the Royal Society of London*, 29, (1879), 71–97.

Roshko, A.: On the Development of Turbulent Wakes from Vortex Streets. *Tech. rep. 1191*. *National Advisory Committee for Aeronautic*, (1954).

Sabrowski, P.; Paschedag, A. R.; Przybilla, S.; Kray, S.; Gutekunst, J.: Smoothed Particle Hydrodynamics – ein neuer Ansatz in der CFD. Jahrestreffen der ProcessNet-Fachgruppen Computational Fluid Dynamics, (2017).

Sun, P. N.; Zhang, A. M.; Colagrossi, A.; Marrone, S.; Antuono, M.: Targeting viscous flows around solid body at high Reynolds numbers with the δ plus-SPH model. *12th International SPHERIC Workshop*, (2017a), 1-8.

Sun, P. N.; Colagrossi, A.; Marrone, S.; Zhang, A. M.: The δ plus-SPH model: simple procedures for a further improvement of the SPH scheme. *Computer Methods in Applied Mechanics and Engineering*, Vol. 315, (2017b), 25-49.

Swope, W. C.; Andersen, H. C.; Berens, P. H.; Wilson, K. R.: A Computer Simulation Method for the Calculation of Equilibrium Constants for the Formation of Physical Clusters of Molecules Application to Small Water Clusters. *The Journal of Chemical Physics*, 78, (1982), 637-649.

Tafuni, A.: Smoothed Particle Hydrodynamics: Development and Application to Problems of Hydrodynamics. *Dissertation*, New York University Tandon School of Engineering, (2016).

Tafuni, A.; Domínguez, J. M.; Vacondio, R.; Crespo, A. J. C.: Accurate and efficient SPH open boundary conditions for real 3-D engineering problems. *12th International SPHERIC Workshop*, (2017), 346-354.

Urso, M. E.; Lawrence, C. J.; Adams, M. J.: Pendular, Funicular, and Capillary Bridges: Results for Two Dimensions. *Journal of colloid and interface science*, 220, (1999), 42–56.

Vacondio, R.; Rogers, B. D.; Stansby, P. K.; Mignosa, P.: Variable resolution for SPH in three dimensions: Towards optimal splitting and coalescing for dynamic adaptivity. *Computer Methods in Applied Mechanics and Engineering*, 300, (2016), 442-460.

Violeau, D.: One and two-equations turbulent closures for Smoothed Particle Hydrodynamics. *Proceedings of the 6th International Conference on Hydroinformatics*, (2004), 87-94.

Violeau, D.: *Fluid Mechanics and the SPH Method Theory and Applications*. Oxford University Press, Oxford (2012).

Violeau, D.; Rogers, B. D.: 2016, "Smoothed particle hydrodynamics (SPH) for freesurface flows: past, present and future", *Journal of Hydraulic Research*, Vol. 54, pp. 1-26.

Watkins, S. J.; Bhattal, A. S.; Francis, N.; Turner, J. A.; Whitworth, A. P.: A new prescription for viscosity in Smoothed Particle Hydrodynamics. *Astronomy and Astrophysics Supplement Series*, 119, (1996), 177–187.

Wendland, H.: Piecewise polynomial, positive definite and compactly supported radial functions of minimal degree. *Advances in Computational Mathematics*, 4, (1995), 389-396.

Addresses: Technische Universität Berlin, Straße des 17. Juni 135, 10623 Berlin
Beuth Hochschule für Technik Berlin, Luxemburger Str. 10, 13353 Berlin
dive solutions GmbH, c/o Maik Störmer, Gudrunstr. 10, 10365
email: pierre.sabrowski@tu-berlin.de
sabine.przybilla@beuth-hochschule.de
pause@dive-solutions.de
lennart.beck@beuth-hochschule.de
villwock@beuth-hochschule.de
paul-uwe.thamsen@tu-berlin.de